RSC Advances

ROYAL SOCIETY OF CHEMISTRY

www.rsc.org/advances

Balanced toughening and strengthening of ethylene-propylene rubber toughened isotactic polypropylene by using poly(styrene-*b*-ethylene/propylene) diblock copolymer

Feng Chen, Biwei Qiu, Bo Wang, Yonggang Shangguan,* Qiang Zheng

MOE Key Laboratory of Macromolecular Synthesis and Functionalization, Department of Polymer Science and Engineering, Zhejiang University, Hangzhou 310027, People's Republic of China

Abstract For ordinary rubber toughened plastics, the introduction of rubber will inevitably bring about the severe decline in mechanical strength due to the low modulus and rigidity of elastomers. To fabricate toughened polypropylene (PP) materials without significant strength degradation, the poly(styrene-*b*-ethylene/propylene) diblock copolymer (SEP) was used as the third component in isotactic polypropylene/ethylene-propylene random copolymer (*i*PP/EPR) to prepare a series of PP/EPR/SEP blends. The phase morphology, dynamic mechanical behavior, crystallization behavior and mechanical property of PP/EPR/SEP blends were systematically investigated, compared with PP/EPR blends. The dynamic mechanical analysis results revealed that SEP has a good compatibility with both EPR phase and amorphous PP phase, which led to an improvement of

*Corresponding authors. Department of Polymer Science and Engineering, Zhejiang University, Hangzhou 310027, PR China. Tel./fax: +86 571 8795 3075.
E-mail: shangguan@zju.edu.cn (YG. Shangguan)

interfacial adhesion between them. The mechanical properties testing results indicated that the introduction of SEP could effectively promote the brittle-ductile transition for PP/EPR blends and that PP/EPR/SEP blends presented a good toughness without strength loss. Considering the fact that the individual EPR or SEP couldn′t achieve the good toughening, it was proposed that SEP and EPR have a synergistic effect on toughening PP and a modified PP with balanced toughness and tensile strength can be achieved by simultaneous adding EPR and SEP into *i*PP.

Key Words: poly(styrene-*b*-ethylene/propylene) diblock copolymer; toughening; synergistic effect

1 Introduction

Polypropylene (PP) is an important thermoplastic due to its wide applications and low cost. However, the poor impact strength especially at low temperatures is one major drawback of PP. Consequently, toughening PP has been an important research issue. Up to now, a great deal of effort has been made to improve the impact property of PP through physical or chemical methods. Due to the simple operation, much attention has been paid to the physical method of adding a variety of elastomers into PP.[1-6] As a result, various modified PP/rubber systems have been prepared, such as PP/ethylene-propylene rubber (EPR),[7,8] PP/ethylene-propylene-diene monomer (EPDM)[9-11] and PP/styrene-butadiene-styrene (SBS) or styrene-ethylene/1-butene-styrene (SEBS) block copolymers.[12-15] Correspondingly, different toughening mechanisms have been proposed.[2,16-19] However, it is well

accepted that the rubber inclusions can play the role of agent-induced crazing, cause shear yielding of the matrix around them, and end the propagation of cracks, resulting in significantly higher toughness of modified PP than neat PP.[20]

Due to the low cost and availability, PP/EPR has been one of the most important modified PP products. It is believed that rubber phase with smaller average particle diameter *d* seems to be more efficient in toughening.[21-24] That fact indicates the dispersion of rubber in PP matrix has an important influence on the toughness of end products. However, since phase separation takes place in PP/EPR at temperatures above melting point of PP-crystals, inevitable phase coarsening during melt processing will results in some unexpected performance degradations.[25-27] In order to improve the interfacial adhesion and stabilize the phase structure, EPR modified by maleic anhydride (MA) was used as the compatibilizer.[28] It was reported that the grafted EPR with MA could decrease the rubber particle size from 1.05 to 0.34 μm and improve the impact strength of the blends. On the other hand, due to the higher service temperature and better solvent resistance, PP blends with thermoplastic elastomers (TPE) like SBS and SEBS hold the promise of improved properties in relation to those obtained using conventional elastomers, leading to a wider scope of applications of these materials.[29]

For ordinary rubber toughened plastics, the low modulus and rigidity of elastomers easily result in a marked decrease in rigidity of end products. That will no doubt cause the limitation of application for the products. However, considering impact polypropylene copolymer (IPC), a popular thermoplastic that exhibits a good

rigidity-toughness balance and is widely used in automotive industry,[30,31] the aim of simultaneous achieving excellent toughness and high rigidity is not unrealistic. In recent years, different polymer materials with combined high toughness and stiffness were produced by several approaches. Bao et al[32] reported a new PP nanocomposite showing simultaneously enhanced toughness and tensile strength by using a kind of novel β-nucleating agent supported onto the surface of octadecylamine functionalized graphene oxide. Chen et al[33] also demonstrated the hierarchical structure of glass fiber obtained by shear flow and a β-nucleating agent could simultaneously improve the strength and toughness of PP matrix. Other works have also reported that polymer materials with high strength and toughness can be produced by controlling thermally induced self-assembly of β-nucleating agent,[34] and blending with nanoparticle-plasticizers.[35]

In this paper, the poly(styrene-*b*-ethylene/propylene) diblock copolymer (SEP) was used as the third component in PP/EPR system to fabricate highly toughened PP blends without significant strength loss. The phase morphology, thermal behavior, dynamic mechanical behavior and mechanical properties were investigated systematically, and the synergistic effect of EPR and SEP on toughening PP was studied.

2 Experimental

2.1 Materials and sample preparation

The commercial isotactic polypropylene (*i*PP, T300, M_w=3.6×10^5, M_w/M_n=4.23,

Shanghai petrochemical, China), EPR (J-0030, M_w=1.5×10^5, M_w/M_n=2.03, molar percentage of ethylene content is about 45%, Jilin chemical industrial company limited, China), IPC (SP179, M_w=1.7 × 10^5, M_w/M_n=3.96, molar percentage of ethylene component is about 13.5%, SINOPEC Qilu Corporation Ltd., China) and SEP (G1702, M_w=1.2×10^5, M_w/M_n=1.07, the styrene/rubber ratio is 28/72 in weight, Kraton Polymers LLC, USA) were adopted. IPC is a multicomponent copolymer, mainly contains three components, *i.e.*, EPR, a series of ethylene propylene block copolymers with different sequence lengths (E*b*P) and propylene homopolymer (*h*PP).[30,36] Kraton G1702 is a clear, linear diblock copolymer composed of polystyrene (PS) block and ethylene-propylene (EP) rubber block produced by hydrogenating styrene-isoprene block copolymer.[37] EP block in SEP is a hydrogenated polyisoprene block and is completely amorphous. The components are weighed as the designed mass ratio and blended in a torque rheometer (XSS-300, KCCK, Shanghai, China) at 180 ^{o}C and 60 rpm for 10min to prepare the PP/EPR, PP/SEP and PP/EPR/SEP blends. Finally, the Charpy impact and tensile test specimens were prepared by compression molding at 180 ^{o}C under 10 MPa for 8 min. During the processing, a small amount of antioxidant (Irganox 1010) was added.

2.2 Impact strength test

The notched Charpy impact test was conducted on a Charpy impact test machine (MTS Systems Co. Ltd., China) according to ISO 179-1: 2000. A 45° V shaped notch was made (depth 2 *mm*) before measurement. The specimens were kept in an environment container at -20 ^{o}C and 23 ^{o}C for 12 *h* before test, and then immediately

subjected to test. The test result was an average of at least eight specimens.

2.3 Tensile properties test

Tensile tests were performed to dumbbell-shaped samples on a universal testing machine (CMT 4204, Shenzhen SANS Test Machine Co. Ltd., China) at 50 mm/min at room temperature ((25 ± 3) ºC). Mechanical properties were determined from five replicates for each sample.

2.4 Scanning electron microscope observation

The fracture surface of specimens obtained at liquid nitrogen was etched in 50 ^{o}C *n*-octane for 4 *h* (or in 50 ^{o}C toluene for 4 *h*, for the inserts in **Fig. 4**), and observed using a scanning electron microscope (SEM, S-4800, Hitachi, Japan) after being coated with gold-palladium. The operating voltage was 3 kV.

2.5 Dynamic mechanical analysis measurement

The dynamic mechanical analysis (DMA) measurements were carried out on a Q800 analyzer (TA Instruments Corporation, USA). The single cantilever mode was used, and the measurement was carried out from -140 ^{o}C to 130 ^{o}C at a heating rate of 3 ^{o}C/min and an oscillatory frequency of 1 Hz.

2.6 Differential scanning calorimetry measurement

The thermal behavior of the blend samples were examined by using a Q100 differential scanning calorimetry (DSC, TA Instruments Corporation, USA) with nitrogen as purge gas. The samples were first heated to 190 ^{o}C and held for 5 min to eliminate previous thermal history, and then cooled down to 40 ^{o}C and maintained for 5 min. Finally, the samples were heated to 190 ^{o}C again. The cooling and the second

heating flow curves were recorded as the thermal behavior. Both the heating and cooling rates in all tests were 10 ^{o}C/min.

3 Results and discussion

3.1 Structure and properties of PP/EPR

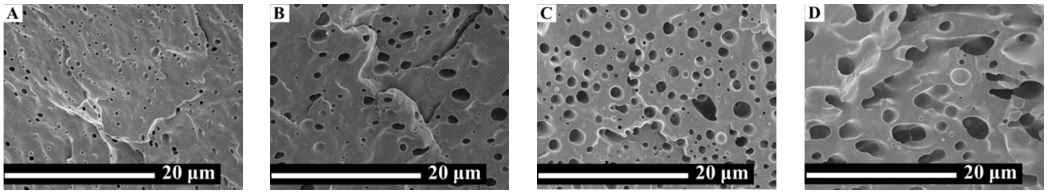

Fig. 1. SEM images of PP/EPR blends with different EPR content. (A) 10%, (B) 20%, (C) 30% and (D) 40%.

As discussed in *Introduction* section, EPR is a widely used elastomer for toughening PP. Here, the phase structure and mechanical properties of PP/EPR binary blends with different EPR content were investigated. **Fig. 1** gives the morphology images of different PP/EPR samples. It can be seen that EPR presents a good dispersion in PP matrix. The size of EPR particles increases monotonically with the increase of EPR content. **Fig. 2** gives the corresponding mechanical properties of various blend samples. As shown in **Fig. 2A**, both the impact strengths at 23 ^{o}C (room temperature) and at -20 ^{o}C (low temperature) increase with the increase of EPR content, which accords with others′ results.[7] However, due to the low modulus and rigidity of rubber, the addition of EPR results in the visible decreases of elastic modulus and tensile strength, as seen in **Fig. 2B**.

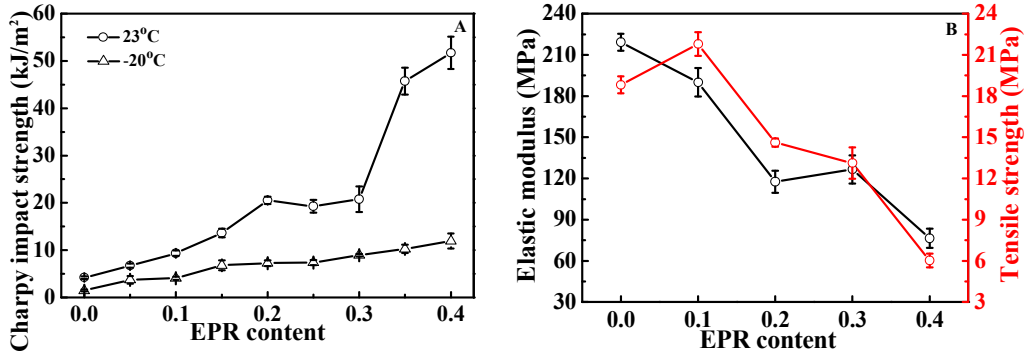

Fig. 2. (A) Impact strength and (B) tensile properties of PP/EPR blends with different EPR content.

Generally speaking, the dynamic mechanical properties are responsible for the reflection on the periodic stress and the storage modulus can also be an indicator of the rigidity to some extent. **Fig. 3** gives the storage moduli and tensile properties of IPC and PP/EPR blends at different temperatures. As similar to tensile properties, the storage modulus of PP/EPR decreases with increasing the EPR content though the extent of reduction for storage modulus is smaller than that for tensile properties. The blend with 30% EPR seems to show a storage modulus similar to IPC in the investigated temperature range, while its impact strength at room temperature is much lower. The impact strength of IPC obtained at room temperature is 51.1 kJ/m^2,[38] 146% higher than that of PP/EPR with 30% rubber content here. Considering the fact that IPC just contains about 19% rubber content,[39] the toughening efficiency of rubber in IPC is much higher than in PP/EPR. The insert shows the tensile properties of IPC and PP/EPR blends. It can be seen that the PP/EPR with 30% rubber exhibits slightly higher elastic modulus and tensile strength than IPC, while PP/EPR with 40% rubber content shows worse tensile properties. Considering the importance of stiffness of end products for application, here PP/EPR with 30% rubber is selected as the matrix. The third component, *i.e.*, SEP, was added into the matrix for the purpose of obtaining the

materials with a good rigidity-toughness balance. For convenience, the PP/EPR with 30% rubber is defined as PPM in this paper later.

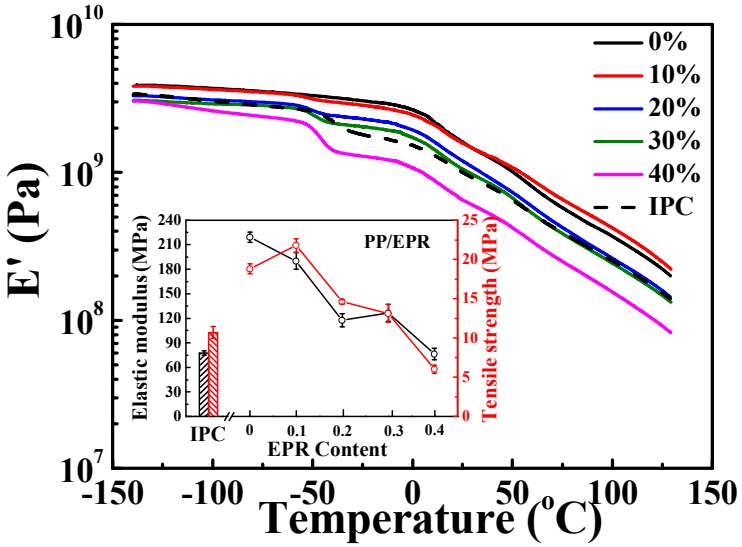

Fig. 3. Storage modulus of IPC and PP/EPR blends with different EPR content. The insert shows the corresponding elastic modulus and tensile strength of these samples.

3.2 Compatibilizing Effect of SEP on PPM

The phase morphologies of various PPM/SEP blends are displayed in **Fig. 4**. As seen from these images, the rubber size seems to maintain a constant as increasing the SEP content. For the blends with SEP content below 10%, the dispersion of rubber in PP matrix is so fine that there is scarcely any aggregate of rubber phase. However, in the case of SEP content above 10%, the dispersion of rubber seems to be inhomogeneous and the holes resulting from the extraction of rubber in *n*-octane never appear uniformly. This result can be ascribed to that SEP is a diblock copolymer composed of PS segment and EP rubber segment, and the molecular chain with long PS block cannot be removed by *n*-octane at 50 °C. Thus, as the increase of

SEP content, the content of the rubber which can be removed becomes lower, leading to the fewer holes in the SEM images. We have also used toluene as the etching solvent so as to remove both EPR and SEP thoroughly. The images are shown as the inserts in **Fig. 4**. It can be seen that the holes are homogeneous again after removing SEP and EPR, indicating the dispersion of EPR is still fine after adding SEP. In general, it is believed that PP and PS are immiscible and their blend shows a two-phase structure.[40] As a result, there are sharp interfaces between PP matrix and PS dispersed phase, showing the poor adhesion between different phases.[41,42] However, in our case, the interfaces between PP matrix and PS domain are hardly seen, indicating there is a good compatibility between the two phases due to the existence of EP segment.

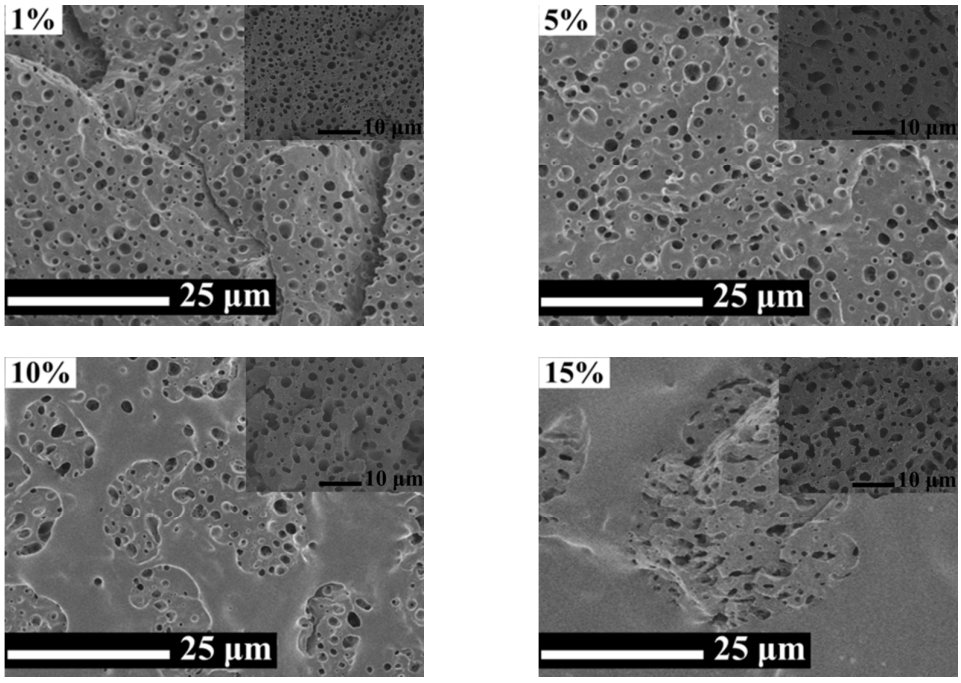

Fig. 4. SEM images of PPM/SEP blends with different SEP content. The inserts were obtained by recording the samples etched in 50 ^{o}C toluene for 4 *h*.

It is believed that the dynamic mechanical analysis (DMA) can be used to evaluate the mobility of molecular chains in polymer system. Here, the PPM/SEP blends were measured by DMA and the corresponding results are given in **Fig. 5**. For all blends, there are three distinct damping peaks. The peak at about -48 ^{o}C is related to the glass transition of rubber phase; the peak at about 15 ^{o}C is related to the β-relaxation of PP (the glass transition of amorphous PP) and the peak at about 90 ^{o}C is related to the α-relaxation of PP (the relaxation of restricted amorphous PP chains in the crystalline phase or known as rigid amorphous molecules).[43] However, since the glass transition temperature (T_g) of PS is at about 100 ^{o}C,[42,44] the peak at about 90 ^{o}C here may be simultaneously contributed by the α-relaxation of PP and the glass transition of PS segment. As seen from the partially enlarged view, with the increase of SEP content, the peak temperatures of rubber relaxation and PP β-relaxation shift towards each other. In addition, the peak at about 90 ^{o}C also shifts towards the lower temperature. Since there are multiple components in these blends, *i.e.*, amorphous EPR phase, amorphous PP phase, crystalline PP phase, EP domain of SEP and PS domain of SEP, the interactions among these phases are complex. Moreover, in the case of the SEP content above 5%, the fourth damping peak can be observed at about -75 ^{o}C, as shown by the orange arrow. While the SEP content is below 5%, the peak at -75 ^{o}C disappears.

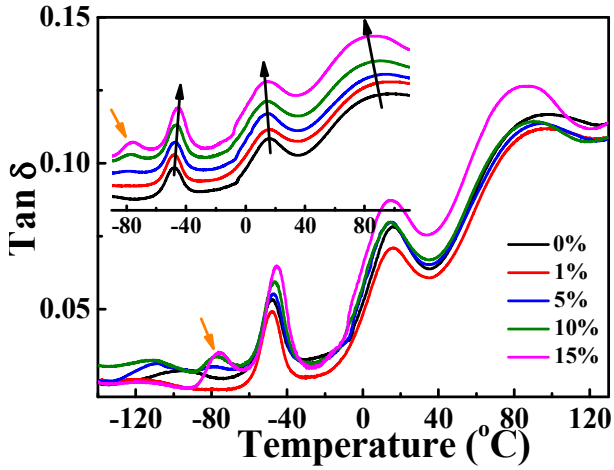

Fig. 5. Dynamic mechanical properties of PPM/SEP blends with different SEP content. The insert shows the partially enlarged view.

In order to study the mobility of molecular chains further, the dynamic mechanical properties of PP/EPR and PP/SEP binary blends are shown in **Fig. 6**. As for PP/EPR blends, the three damping peaks stand for the EPR relaxation at about -48 °C, *β*-relaxation of PP at about 15 °C and α-relaxation of PP at about 90 °C, respectively. While for PP/SEP blends, the damping peaks at about -75 °C, 15 °C and 90 °C are responsible for the relaxations of EP domain, amorphous PP phase and rigid amorphous PP phase (also the PS domain), respectively. As seen in **Fig. 6A**, the EPR relaxation temperature rises with the increase of EPR content, while the peak temperatures of α-relaxation and *β*-relaxation for PP phase are unchanged. For the polymer blends with phase-separated structures, the glass transition temperatures of components will shift towards each other in the partially miscible polymer blends or remain unchanged in the completely immiscible polymer blends.[45,46] Thus, the T_g shifting of only one component in binary blends never results from the compatibility. In our another work, we have also found the glass transition temperature of EPR in

PP/EPR binary blend increases with increasing EPR content, while the glass transition temperatures of PP are unchanged.[47] We have studied this issue carefully and proved that it results from the mismatch of thermal expansion coefficients of the two components (seen in supporting information). For PP/SEP blends, the introduction of SEP leads to the shift towards each other of loss peak temperatures for EP relaxation and PP β-relaxation, indicating there is a relatively good compatibility between EP domain and amorphous PP phase. Moreover, the loss peak at about 90 ^{o}C also shifts towards lower temperature as the increase of SEP content. As pointed out above, the loss peak at about 90 ^{o}C is contributed by the relaxation of restricted amorphous PP chains in the crystalline phase and relaxation of PS domain. Considering the fact that the molecular chains of other components hardly enter into the crystalline PP phase, the temperature of PP-α relaxation is usually unchanged. Thus, it is reasonable that this shift towards lower temperature of the loss peak at about 90 ^{o}C should be contributed by the PS relaxation. Due to the existence of EP domain which can play the role of compatibilizer between amorphous PP and PS domain, the molecular chains of amorphous PP and PS can infiltrate into each other to some extent, leading to the shift towards lower temperature of loss peak for PS relaxation. Consequently, the changes of the three peak temperatures in **Fig. 5** should result from the relatively good compatibility between amorphous PP phase and rubber phase, also between amorphous PP phase and PS domain. On the other hand, the glass transition temperature of EP domain in **Fig. 6B** is at about -75 ^{o}C, much lower than that of EPR phase (at about -48 ^{o}C) in **Fig. 6A**. Thus, when SEP content is above 5%, the forth

damping peak appearing at about -75 °C in **Fig. 5** should be ascribed to the relaxation of EP domain; on the contrary, when SEP content is low, due to the limitation of resolution for the DMA machine, the relaxation of EP domain cannot be detected.

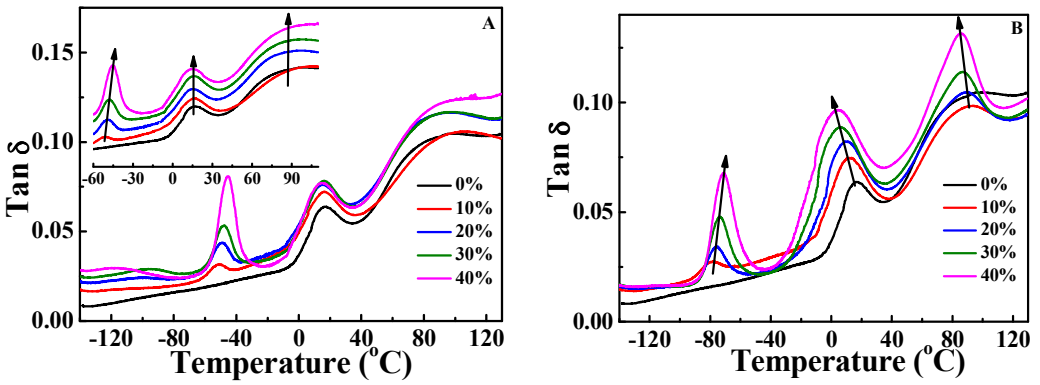

Fig. 6. Dynamic properties of (A) PP/EPR blends with different EPR content and (B) PP/SEP blends with different SEP content. The insert in (A) shows the partially enlarged view.

The relatively good compatibilities between amorphous PP phase and rubber phase and between amorphous PP phase and PS domain no doubt will affect the crystallization behavior of PP and in turn influence the crystal structure. Thus, the crystallization and melting behavior of PPM/SEP blends were investigated and the results are displayed in **Fig. 7**. It can be seen that the temperatures of crystallization peak and melting peak both shift towards lower temperature as the increase of SEP content. Arroyo[48] reported that EPDM at low percentages (<25%) can act as nucleating agent promoting crystallization. However, in our case there is no nucleation effect of SEP considering the decrease of crystallization temperature. For PPM/SEP blends, due to 30% EPR loading in the PPM matrix, the addition of SEP certainly increases amorphous phase content further. The high content of amorphous

phase inevitably brings about a dilution effect on the crystallization of PP since there is a relatively good compatibility between PP and SEP, leading to the shift towards lower temperature of PP crystallization peak. Furthermore, it is believed that there is a local phase separation at the growth front of the spherulites, which is mainly caused by the preferential rejection of impurities during crystallization.[49-51] Due to the good compatibility between PP phase and rubber phase induced by SEP, the increase of SEP certainly enhances the dilution effect on PP crystallization and in turn results in the smaller lamella thickness. So the melting point of PPM/SEP blends decreases with the increase of SEP. However, the variation of the melting point is small and the crystallinity of PP is hardly influenced by SEP, as seen in the insert in **Fig. 7A**.

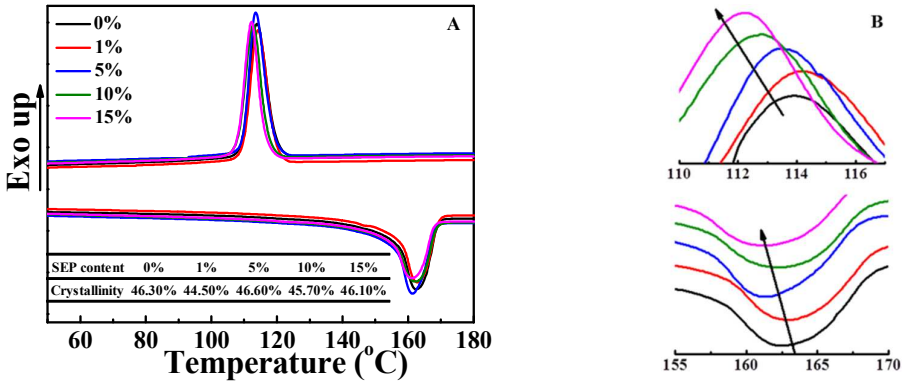

Fig. 7. (A) DSC curves of PPM/SEP blends with different SEP content and (B) the partially enlarged views of crystallization peak and melting peak. The insert in (A) gives the crystallinity of PP for these blends.

3.3 Toughening and strengthening of SEP on PPM

The above results reveal that SEP has a significant effect on improving the compatibility between amorphous PP phase and rubber phase, inhibiting the crystallization behavior though the crystallinity of PP is hardly influenced.

Considering the fact that strong interfacial adhesion favors improving the impact strength of end product, the mechanical properties of PPM/SEP blend is full of promise. **Fig. 8** gives the impact strength of PPM/SEP blends with different SEP content. It can be seen that both the impact strengths at room temperature and low temperature increase with increasing SEP content. For room temperature test, the impact strength increases from 20.8kJ/m^2 to 65.7 kJ/m^2, increased by 216%. As for low temperature test, the impact strength increases from 8.9 kJ/m^2 to 19.6 kJ/m^2, also increased by 120%. These facts mean SEP has a great effect on the toughening of PP/EPR blend. It is amazing that just only a small content of SEP (1%) can result in the much higher impact strength at room temperature, *i.e.*, from 20.8kJ/m^2 to 58.4 kJ/m^2, increased by 181%. When SEP content is above 1%, the impact strength is slightly fluctuant first, and then increases slowly. However, the impact strength at low temperature steadily increases. In view of the much higher price of SEP than that of PP or EPR, the impact strength at room temperature shows an excellent economic value, since just a small amount of SEP can lead to a satisfactory toughness.

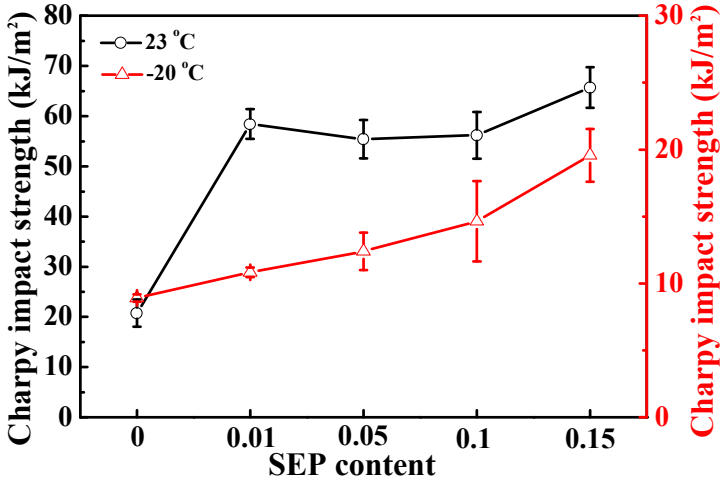

Fig. 8. Impact strength of PPM/SEP blends with different SEP content.

As discussed above, SEP is a linear diblock copolymer composed of PS block and EP rubber block. Considering this molecular structure, SEP itself probably has an toughening effect on PP due to the rubber phase. Thus, it is necessary to confirm that whether the SEP alone has an excellent toughening effect. Here, PP/SEP binary blends were prepared and investigated. The corresponding impact test results are shown in **Fig. 9A**. It is observed that the impact strengths at both two temperatures slowly increase with the increase of SEP. The impact strength at room temperature only increases from 4.2 kJ/m^2 to 8.5 kJ/m^2 as the SEP content reaches 20%, differing from the rapid increase of impact strength for PPM/SEP blends which increases from 20.8 kJ/m^2 to 58.4 kJ/m^2 as the SEP content just reaches 1%. The above results mean the toughening effect of SEP alone is limited, while the simultaneous usages of SEP and EPR can achieve a significant improvement of impact strength of PP. Considering the toughening results of 30% EPR in PP matrix as shown in **Fig. 2**, these results also indicate the increase of impact strength in **Fig. 8** results from a synergistic effect of SEP and EPR. Taking the results revealed in *3.2 section* into account, the significant improvement of impact strength for PPM/SEP blends is reasonably ascribed to the stronger interfacial adhesion resulting from the improvement of compatibility by adding SEP. Due to the relatively good compatibility of SEP with EPR phase and amorphous PP phase, the addition of SEP improves the interfacial adhesion between rubber phase and PP matrix. On the other hand, the PS domain can play a role of physical crosslinking points since the PS domain is in the glass state at room temperature, which also increases the impact strength of end product.

Furthermore, the influence of EPR content on PP/SEP/EPR blends was also investigated, in which the SEP content is fixed at 5%. As seen in **Fig. 9B**, the impact strength at both two temperatures increases with increasing EPR content, which is similar to the results of PP/EPR binary blends, in **Fig. 2A**. However, there is a significant difference in room temperature test that the brittle-ductile transition occurs in PP/EPR binary blends at the EPR content of about 32.5% (as seen in **Fig. 2A**) while it occurs in PP/SEP/EPR blends (the SEP content is determined as 5%) at the EPR content of about 22.5% (as seen in **Fig. 9B**). This fact means that the existence of SEP can effectively decrease the critical EPR content at which the brittle-ductile transition occurs, indicating that the lower rubber content enables the high impact strength. This result is important for manufacturing since high rubber content inevitably decreases the modulus and rigidity of end product. Moreover, the impact strength at EPR content below 20% in **Fig. 9B** is close to that in **Fig. 2A**, indicating that the toughening effect of SEP should work at the EPR content above 20%.

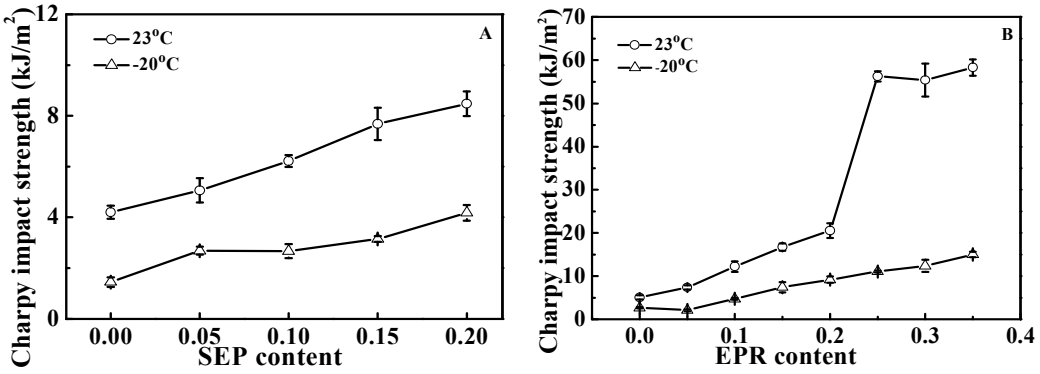

Fig. 9. Impact strength of (A) PP/SEP blends with different SEP content and (B) PP/SEP/EPR blends with different EPR content. For PP/SEP/EPR blend, the SEP content is determined as 5%, and the EPR content is adjusted.

Fig. 10 gives the tensile properties and storage modulus of PPM/SEP blends. It is observed that as increasing SEP content, the elastic modulus, tensile strength and storage modulus basically remains unchanged first and then decreases a little. For the 1% content of SEP, the elastic modulus, tensile strength and storage modulus is basically consistent with that of PPM, respectively. Considering the fact that 1% SEP has already resulted in excellent impact strength, this unchanged rigidity means that SEP can improve the toughness and simultaneously remain the original rigidity of materials. For example, the PPM/SEP blend with 1% SEP possesses the impact strength of 58.4 kJ/m^2, elastic modulus of 144.7 MPa and the tensile strength of 12.6 MPa. However, for PP/EPR binary blend in **Fig. 2**, when the impact strength reaches the value of 51.7 kJ/m^2, still lower than that of PPM/SEP blend, a lower elastic modulus of 76.3 MPa and a tensile strength of 6.0 MPa appear. In a word, the results presented in this work reveal that the combined usage of SEP and EPR have a synergistic effect on toughening PP which is not at the expense of rigidity.

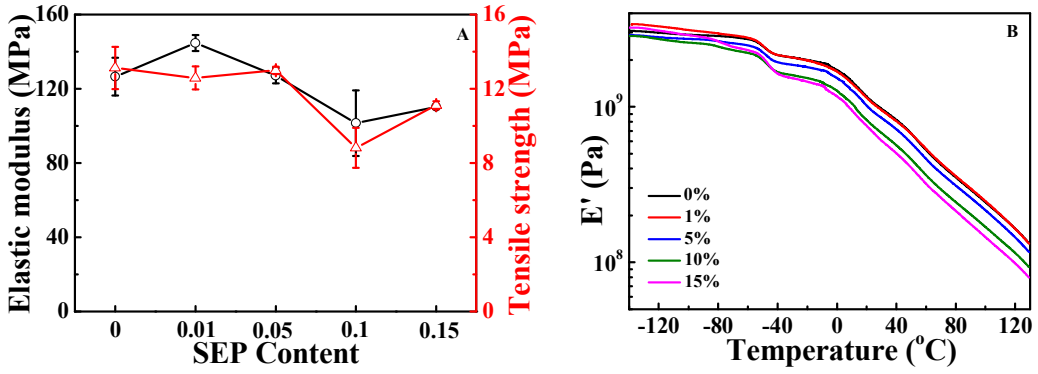

Fig. 10. (A) Tensile properties and (B) storage modulus of PPM/SEP blends with different SEP content.

Conclusions

Dynamic mechanical analysis measurements reveal that SEP has a relatively good compatibility with both EPR phase and amorphous PP phase, leading to the improvement of interfacial adhesion. The addition of SEP decreases the crystallization temperature and melting point of PP, which can be ascribed to the dilution effect. The impact test results indicate that the existence of SEP can effectively promote the brittle-ductile transition for PP/EPR blends by decreasing the critical EPR content. Since EPR or SEP alone could not achieve the excellent toughening effect for PP matrix, it is proposed that SEP and EPR have a synergistic effect on toughening PP and the toughening effect is not at the expense of rigidity.

Acknowledgements

This work was supported by National Nature Science Foundation of China (No. 51173157, 51173165) and the Fundamental Research Funds for the Central Universities (No. 2013QNA4048).

References

1. J. F. Wang, C. L. Wang, X. L. Zhang, H. Wu and S. Y. Guo, RSC Adv., 2014, 4(39), 20297-20307.
2. G. Goizueta, T. Chiba and T. Inoue, Polymer, 1992, **33**(4), 886-888.
3. A. Lazzeri and C. B. Bucknall, Polymer, 1995, **36**(15), 2895-2902.
4. Y. G. Shangguan, L. Y. Tao, L. Zhao, Q. Zheng, Acta Polym. Sinica, 2007, **8**, 770-774
5. A. Margolina and S. H. Wu, Polymer, 1988, **29**(12), 2170-2173.
6. S. C. Wong and Y. W. Mai, Polymer, 1999, **40**(6), 1553-1566.
7. L. Dorazio, C. Mancarella, E. Martuscelli and F. Polato, Polymer, 1991, **32**(7), 1186-1194.
8. G. M. Kim, G. H. Michler, M. Gahleitner and J. Fiebig, J. Appl. Polym. Sci., 1996, **60**(9), 1391-1403.
9. C. Y. Chen, W. Yunus, H. W. Chiu and T. Kyu, Polymer, 1997, **38**(17), 4433-4438.
10. A. van der Wal, R. Nijhof and R. J. Gaymans, Polymer, 1999, **40**(22), 6031-6044.
11. A. van der Wal, J. J. Mulder and R. J. Gaymans, Polymer, 1998, **39**(26), 6781-6787.
12. M. Saroop and G. N. Mathur, J. Appl. Polym. Sci., 1999, **71**(1), 151-161.
13. G. G. Ferrer, M. S. Sanchez, E. V. Sanchez, F. R. Colomer and J. L. G. Ribelles, Polym. Int., 2000, **49**(8), 853-859.
14. S. Setz, F. Stricker, J. Kressler, T. Duschek and R. Mulhaupt, J. Appl. Polym. Sci., 1996, **59**(7), 1117-1128.
15. M. Saroop and G. N. Mathur, J. Appl. Polym. Sci., 1997, **65**(13), 2691-2701.
16. Y. H. Wang, X. L. Xu, J. Dai, J. H. Yang, T. Huang, N. Zhang, Y. Wang, Z. W. Zhou and J. H. Zhang, RSC Adv., 2014, 4(103), 59194-59203.
17. D. A. Shi, E. W. Liu, T. Y. Tan, H. C. Shi, T. Jiang, Y. K. Yang, S. F. Luan, J. H. Yin, Y. W. Mai and R. K. Y. Li, RSC Adv., 2013, 3(44), 21563-21569.
18. S. H. Wu, Polymer, 1985, **26**(12), 1855-1863.
19. Y. Guo, S. L. Sun and H. X. Zhang, RSC Adv., 2014, 4(102), 58880-58887.
20. J. Z. Liang and R. K. Y. Li, J. Appl. Polym. Sci., 2000, **77**(2), 409-417.
21. W. M. Speri and G. R. Patrick, Polym. Eng. Sci., 1975, **15**(9), 668-672.
22. R. H. Beck, S. Gratch, S. Newman and K. C. Rusch, J. Polym. Sci., Part B: Polym. Lett., 1968, **6**(10PB), 707-709.
23. A. Pavan and T. Ricco, J. Mater. Sci., 1976, **11**(6), 1180-1182.
24. B. Z. Jang, J. Appl. Polym. Sci., 1985, **30**(6), 2485-2504.
25. N. Inaba, K. Sato, S. Suzuki and T. Hashimoto, Macromolecules, 1986, **19**(6), 1690-1695.
26. L. D'Orazio, C. Mancarella, E. Martuscelli, G. Cecchin and R. Corrieri, Polymer, 1999, **40**(10), 2745-2757.
27. L. Y. Tao, Y. G. Shangguan, X. Jiang, Q. Zheng, Acta Polym. Sinica, 2008, **1**, 48-54
28. M. Mehrabzadeh and K. H. Nia, J. Appl. Polym. Sci., 1999, **72**(10), 1257-1265.
29. F. Abreu, M. M. C. Forte and S. A. Liberman, J. Appl. Polym. Sci., 2005, **95**(2), 254-263.
30. C. H. Zhang, Y. G. Shangguan, R. F. Chen, Y. Z. Wu, F. Chen, Q. Zheng and G. H. Hu, Polymer, 2010, **51**(21), 4969-4977.
31. B. W. Qiu, F. Chen, Y. G. Shangguan, L. N. Zhang, Y. Lin and Q. Zheng, RSC Adv., 2014, **4**(103), 58999-59008.

32. R. Y. Bao, J. Cao, Z. Y. Liu, W. Yang, B. H. Xie and M. B. Yang, J. Mater. Chem. A, 2014, 2(9), 3190-3199.
33. Y. H. Chen, Z. Y. Huang, Z. M. Li, J. H. Tang and B. S. Hsiao, RSC Adv., 2014, 4(28), 14766-14776.
34. Y. J. Li, X. Y. Wen, M. Nie and Q. Wang, J. Appl. Polym. Sci., 2014, **131**(16), 40605.
35. B. Yin and M. Hakkarainen, J. Mater. Chem., 2011, **21**(24), 8670-8677.
36. R. F. Chen, Y. G. Shangguan, C. H. Zhang, F. Chen, E. Harkin-Jones and Q. Zheng, Polymer, 2011, **52**(13), 2956-2963.
37. H. S. Yu, J. H. Wang, A. Natansohn and M. A. Singh, Macromolecules, 1999, **32**(13), 4365-4374.
38. F. Chen, B. W. Qiu, Y. G. Shangguan, Y. H. Song and Q. Zheng, Mater. Des., 2015, 69, 56-63
39. F. Chen, B. W. Qiu, Y. H. Lv, Y. G. Shangguan and Q. Zheng, RSC Adv., 2014, **4**(101), 57935-57944.
40. F. You, D. R. Wang, X. X. Li, M. J. Liu, Z. M. Dang and G. H. Hu, J. Appl. Polym. Sci., 2014, **131**(13), 40455
41. N. Wang, N. Gao, Q. H. Fang and E. F. Chen, Mater. Des., 2011, **32**(3), 1222-1228.
42. J. G. Li, H. Y. Li, C. H. Wu, Y. C. Ke, D. J. Wang, Q. Li, L. Y. Zhang and Y. L. Hu, Eur. Polym. J., 2009, **45**(9), 2619-2628.
43. C. Grein, K. Bernreitner and M. Gahleitner, J. Appl. Polym. Sci., 2004, **93**(4), 1854-1867.
44. S. G. Lee, J. H. Jae, K. Y. Choi and J. M. Rhee, Polym. Bull., 1998, **40**(6), 765-771.
45. J. H. Lee and S. C. Kim, Macromolecules, 1986, **19**(3), 644-648.
46. A. K. Gupta, V. B. Gupta, R. H. Peters, W. G. Harland and J. P. Berry, J. Appl. Polym. Sci., 1982, **27**(12), 4669-4686.
47. F. Chen, B. W. Qiu, G. H. Luo, Y. G. Shangguan and Q. Zheng, 2015, **submitted**
48. M. Arroyo, R. Zitzumbo and F. Avalos, Polymer, 2000, **41**(16), 6351-6359.
49. H. Tanaka and T. Nishi, Phys. Rev. A, 1989, **39**(2), 783-794.
50. H. Tanaka and T. Nishi, Phys. Rev. Lett., 1985, **55**(10), 1102-1105.
51. D. Cheng, J. C. Feng and J. J. Yi, J. Appl. Polym. Sci., 2012, **123**(3), 1784-1792.